Polynomial scaling approximations and dynamic correlation corrections to doubly occupied configuration interaction wave functions

Mario Van Raemdonck, Diego R. Alcoba, Ward Poelmans, Stijn De Baerdemacker, Alicia Torre, Luis Lain, Gustavo E. Massaccesi, Dimitri Van Neck, and Patrick Bultinck

Citation: The Journal of Chemical Physics **143**, 104106 (2015); doi: 10.1063/1.4930260
View online: http://dx.doi.org/10.1063/1.4930260
View Table of Contents: http://scitation.aip.org/content/aip/journal/jcp/143/10?ver=pdfcov
Published by the AIP Publishing

Polynomial scaling approximations and dynamic correlation corrections to doubly occupied configuration interaction wave functions

Mario Van Raemdonck,[1,a)] Diego R. Alcoba,[2] Ward Poelmans,[3] Stijn De Baerdemacker,[1] Alicia Torre,[4] Luis Lain,[4] Gustavo E. Massaccesi,[5] Dimitri Van Neck,[3] and Patrick Bultinck[1,b)]

[1]*Department of Inorganic and Physical Chemistry, Ghent University, Krijgslaan 281 (S3), 9000 Gent, Belgium*
[2]*Departamento de Física, Facultad de Ciencias Exactas y Naturales, Universidad de Buenos Aires and Instituto de Física de Buenos Aires, Consejo Nacional de Investigaciones Científicas y Técnicas, Ciudad Universitaria, 1428 Buenos Aires, Argentina*
[3]*Center for Molecular Modeling, Ghent University, Technologiepark 903, 9052 Zwijnaarde, Belgium*
[4]*Departamento de Química Física, Facultad de Ciencia y Tecnología, Universidad del País Vasco, Apdo. 644, E-48080 Bilbao, Spain*
[5]*Departamento de Ciencias Exactas, Ciclo Básico Común, Universidad de Buenos Aires, Ciudad Universitaria, 1428 Buenos Aires, Argentina*

(Received 2 July 2015; accepted 26 August 2015; published online 11 September 2015)

A class of polynomial scaling methods that approximate Doubly Occupied Configuration Interaction (DOCI) wave functions and improve the description of dynamic correlation is introduced. The accuracy of the resulting wave functions is analysed by comparing energies and studying the overlap between the newly developed methods and full configuration interaction wave functions, showing that a low energy does not necessarily entail a good approximation of the exact wave function. Due to the dependence of DOCI wave functions on the single-particle basis chosen, several orbital optimisation algorithms are introduced. An energy-based algorithm using the simulated annealing method is used as a benchmark. As a computationally more affordable alternative, a seniority number minimising algorithm is developed and compared to the energy based one revealing that the seniority minimising orbital set performs well. Given a well-chosen orbital basis, it is shown that the newly developed DOCI based wave functions are especially suitable for the computationally efficient description of static correlation and to lesser extent dynamic correlation. © *2015 AIP Publishing LLC.* [http://dx.doi.org/10.1063/1.4930260]

I. INTRODUCTION

The exact solution of the Schrödinger equation[1,2] for an N-electron system is given, within any basis set, by the full configuration interaction (FCI) procedure. Unfortunately, the FCI method is usually intractable except for small systems. Typically, the computational cost is reduced by incorporating only a selected set of N-electron Slater determinants in the configuration interaction (CI) wave functions, leading to the so-called truncated CI methods, for example, CI with only single and double (CISD) electron excitations. These excitations are defined with respect to a given reference, e.g., the restricted Hartree-Fock (RHF) determinant.[2] This kind of methods is typically well suited to account for dynamic correlation as they are closely related to performing perturbation theory around a good reference state. A different way of reducing the FCI space is by projecting the wave function only on the determinants with a specified seniority number, where the seniority number equals the number of singly occupied orbitals in a determinant.[3] The seniority number operator may be formulated as

$$\hat{\Omega} = \sum_{i,\sigma} a^{\dagger}_{i\sigma} a_{i\sigma} - \sum_{i,\sigma_1,\sigma_2} a^{\dagger}_{i\sigma_1} a^{\dagger}_{i\sigma_2} a_{i\sigma_2} a_{i\sigma_1}, \tag{1}$$

where $a^{\dagger}_{i\sigma}$ creates a particle in the ith orbital of an orthonormal basis with spin σ (α or β type) and $a_{i\sigma}$ is the corresponding annihilation operator. In terms of reduced density matrices, the expectation value of the seniority number operator can be obtained as

$$\begin{aligned}\left\langle \hat{\Omega} \right\rangle &= \langle \Psi | \hat{\Omega} | \Psi \rangle \\ &= \sum_i \gamma_{i,i} - 2 \sum \Gamma_{ii,ii},\end{aligned} \tag{2}$$

where $\sum_i \gamma_{i,i}$ is the trace over the first-order spin summed reduced density matrix γ, which equals the number of electrons N, and $\sum_i \Gamma_{ii,ii}$ is the partial trace of the second order spin-summed reduced density matrix (2-RDM) Γ. The Doubly Occupied Configuration Interaction (DOCI) method is an example of this class of seniority number based methods, as it lies in the seniority zero sector of the FCI wave function.[4,5] For a system with L orbitals, and $K = \frac{N}{2}$ electron pairs, the

a)Electronic mail: mariovr5@hotmail.com
b)Electronic mail: Patrick.Bultinck@UGent.be

DOCI wave function is given by

$$|\Psi_{\mathrm{DOCI}}\rangle = \sum_{j=1}^{\binom{L}{K}} c_j \prod_{i=1}^{K} S^{\dagger}_{\mathbf{j}(i)} |\theta\rangle, \tag{3}$$

where $|\theta\rangle$ is the pair vacuum, and $S_i^{\dagger} = a^{\dagger}_{i\alpha} a^{\dagger}_{i\beta}$ are the pair creation operators in the ith orbital. Each j value corresponds to a vector $\mathbf{j}$ that refers to the string of doubly occupied orbitals for all K pairs. The complexity of a DOCI wave function is much reduced compared to a FCI wave function and therefore comes with a lower computational cost. The interest in DOCI wave functions for chemical purposes lies in its connections with geminal-based theories for chemical bonding.[6] From a FCI point of view, DOCI is a singlet wave function that is able to describe any possible pairing structure of the chemical bond. As a matter of fact, recent calculations[4] have established that DOCI wave functions are perfectly suited to capture the static correlations associated to chemical bonds. Furthermore, DOCI wave functions are size extensive. Unfortunately, several problems remain with the DOCI method. Although the number of determinants expanding the DOCI wave function is strongly reduced compared to that of the FCI wave function, the factorial scaling persists. The first goal of this paper is to examine whether truncated DOCI solutions give comparably good quality results at polynomial scaling computational cost. Reduced-cost DOCI solutions have previously been obtained either by a projected Schrödinger equation approach[7,8] or by using exactly solvable models[9] or a variant of the variational 2-RDM method projected on the seniority zero sector of the Hilbert space.[10]

DOCI performs well at accounting for static correlation but fails in describing dynamic correlation[4] whereas CISD wave functions perform rather well for the latter.[2] A second aim of the paper is therefore to establish how methods based on the union of truncated DOCI and truncated one-electron excitations based CI spaces perform for both types of electron correlation at reduced computational cost. We report several DOCI variants and examine the quality of the corresponding wave functions by computing not only their corresponding energies but also their overlap with more advanced wave functions.

An important feature that is typical for non-FCI wave functions is that their quality depends on the single-particle basis chosen. FCI wave functions always lead to equivalent wave functions irrespective of the (orthonormal) basis chosen, be it, e.g., natural orbitals, RHF molecular orbitals, or any other orthonormal basis. This is no longer true for approximate wave functions such as DOCI and its variants. Hence, there is a need to find the solution with the lowest energy obtainable through a unitary transformation of the orthonormal orbitals. Another aim of the paper is therefore to develop an orbital optimisation algorithm well suited to escape from local energy minima. A good candidate for this purpose was found to be simulated annealing (SA).[11] Although the SA procedure works very well for small systems, we found that it is not practically usable in those cases where the number of active orbitals or electrons is large ($N > 20$), so we also propose a new orbital basis suitable for DOCI and its variants. Some of us have previously shown that the orbital basis that minimises the seniority number of a FCI wave function can be used to achieve a more compact determinantal expansion, where the determinants with zero seniority number are the dominant contributions to the FCI wave function.[12] In practice, this means that this orbital basis can be used as a good approximation to the energy optimised DOCI orbitals. As FCI wave functions are hardly tractable for larger systems, we examine whether a seniority number minimising basis derived from a truncated CI wave function serves equally well.

The different wave functions corresponding to the methods reported in this paper can be elegantly summarised using the Venn diagram in Fig. 1. In all cases, a bar ($\bar{}$) notation means that each excitation involves two paired electrons. CI$\bar{\mathrm{S}}$, for example, means that only excitations of a single electron pair with respect to a closed-shell reference Slater determinant are considered, whereas CISD$\bar{\mathrm{D}}$ means that all single and double electron excitations plus all double electron-pair excitations are taken into account. CI$\bar{\mathrm{S}}$ is therefore a subset of CID, CISD$\bar{\mathrm{D}}$ is a subset of CISDQ, etc. In Fig. 1, the green circle stands for the DOCI space which comprises up to $\bar{K}$ electron-pair excitations, and the yellow ellipse underneath for the CISD space. The intersection of the DOCI and the CISD spaces is the CI$\bar{\mathrm{S}}$ space. Furthermore, we can distinguish within the DOCI space the double electron-pair excitations (with respect to the same reference as the CISD determinants). We will also discuss hybrid methods that consider the union of DOCI and truncated CI spaces, such as CISD, which will be denoted as (CISD ∪ DOCI), and are contained in the red boundary, and the polynomial scaling approximate hybrid methods such as CISD$\bar{\mathrm{D}}$, enclosed by a blue dotted line. All methods from Fig. 1 can be used with any choice of (orthonormal) orbitals. We choose for either molecular orbitals as obtained from a preceding Self Consistent Field (SCF) calculation, (globally) energy optimised orbitals by means of SA or seniority number minimising orbitals.

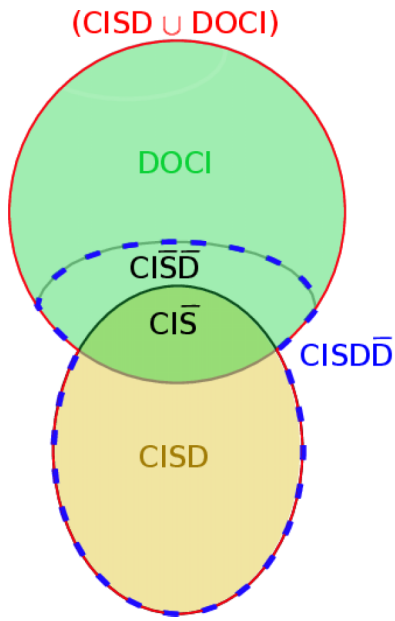

FIG. 1. Overview of the wave functions used for approximations and extensions of the DOCI wave function.

II. ALGORITHMS

A. Computational details and CI solver

In order to assess the accuracy of the methods reported in Section I, we consider the symmetric bond stretching of the BeH_2, H_2O, and N_2 molecules, which are standard tests for methods that aim at describing strongly correlated systems. The used atomic basis sets range from minimal STO-3G to split valence cc-pVDZ. The use of minimal basis sets is considered appropriate here given the nature of the methods tested. All one- and two-particle integrals needed are generated by the PSI4 package.[13] For the interface with PSI4, we used the Hamiltonian class of CheMPS2.[14,15]

For all DOCI, truncated DOCI, and hybrid DOCI calculations, a general CI solver is used that takes as argument a list of Slater determinants. These Slater determinants, in turn, are built from an orthonormal set of orbitals that may correspond to molecular orbitals or some other orthonormal set. All determinants are encoded as binary strings in terms of this set and the Hamiltonian is represented in the Slater determinant basis. The variational problem of determining the Slater determinant coefficients is solved using an implicitly restarted Arnoldi algorithm[16] to locate the chosen number of low lying energy states. All potential energy curves reported below describe the ground state.

B. Orbital optimisation algorithms

DOCI and its variants depend on the chosen orthonormal orbital basis used in the Slater determinants entering the CI expansion. Limacher *et al.*[17] have shown that the basis-dependent DOCI energy surface has many local minima. To cope with those local minimum problems, we now introduce an orbital optimisation algorithm tailored at locating the global energy minimum. For this, the simulated annealing algorithm is chosen as an orbital optimiser. Such techniques have been used previously in quantum chemistry[18] albeit to limited extent, often because of their prohibitive computational cost. Here, such calculations are nevertheless used whenever feasible because they give good benchmark results.

1. Energy based orbital optimisation through simulated annealing

SA is a probabilistic method introduced by Kirkpatrick *et al.*[11] for finding the global minimum of a cost function that may possess several local minima. It does so by emulating the physical process where a solid is gradually cooled and eventually freezes in a minimum energy configuration. This method performs particularly well when there are many local energy minima, as in the case of DOCI wave functions.[17] The work flow for the SA procedure pertaining to the orbital optimisation of CI methods is depicted in Fig. 2. In our implementation, we perform a sequence of elementary Jacobi rotations[19] between randomly selected pairs of orbitals over a randomly chosen angle α. These rotations result in a new orthonormal basis that yields a new energy value. The new basis is then, depending on its energy, accepted or rejected with a certain probability depending on a "temperature" T. The rotation angles α are drawn from a normal distribution around zero and are limited to the interval $[-\alpha_{\max}, \alpha_{\max}]$. Both the temperature T and the maximal angle $\alpha_{\max}$ decrease in the consecutive steps. The starting temperature T is chosen high enough to explore the entire energy surface. Based on our experience, a good choice is $T = 0.5\ E_h$. The rate at which T decreases after each step is chosen as $\delta T = 0.99$. For $\alpha_{\max}$, an initial value $\alpha_{\max} = 1.4$ rad is chosen, and the rate of decrease of the maximum angle is set to $\delta\alpha_{\max} = 0.9999$ as we have found that it is convenient to decrease the maximum angle very slowly so that the flexibility to escape local minima remains. This process is repeated until convergence. For simplicity, we initialise the same T, α_{max}, δT, $\delta\alpha_{max}$ for all pairs of orbitals.

After the rotation of two orbitals, the energy is calculated (E_{new}) with the chosen level of theory and compared to the energy of the previous orbital configuration (E_{old}). If $E_{new} < E_{old}$, the change in the orbitals is always accepted. If $E_{new} \geq E_{old}$, a uniform random number $R_{0,1}$ between zero and one is drawn, and if

$$R_{0,1} < \frac{\exp\frac{E_{old}-E_{new}}{T}}{\exp\frac{E_{old}-E_{new}}{T}+1}, \tag{4}$$

the change is also accepted. This means that the energy may occasionally increase which helps escaping local minima. When T has lowered sufficiently, the chances of such energy increases become negligibly small.

After each step i, the temperature and maximum rotation angle are reduced for the next step $i+1$,

$$T^{(i+1)} = T^{(i)}\delta T, \tag{5}$$

$$\alpha_{max}^{(i+1)} = \alpha_{max}^{(i)}\delta\alpha_{max}. \tag{6}$$

At the end of each cycle, two convergence criteria are checked.

1. Has the maximum number of cycles been reached (here 20 000)?
2. Has the maximum number of consecutive non-acceptance steps been reached (here 1000)?

If one of them is fulfilled, the simulated annealing loop is stopped. Otherwise, the procedure is repeated.

In order to increase the chances of locating the global minimum, several separate SA calculations are performed and the optimal unitary matrix and energy are selected. After this, an extra SA run is performed with very low T and very small maximum angle, in order to locally optimise the minimum further. Our calculations point out that the SA procedure is very effective, as it consistently produces lower energies than those obtained from methods using the orbital gradient and Hessian or the generalised Brillouin theorem.[2,20–22] The SA results may therefore serve as a benchmark for other optimisation schemes.

In practice, we first perform all DOCI and related calculations using Hartree-Fock molecular orbitals, and henceforth, results obtained using this basis are labelled with the caption molecular orbital (MO). Subsequently, the orbital basis is optimised. A first SA procedure allows only rotations among orbitals that belong to the same irreducible representation. Results using this optimised basis are denoted by OO. In a second procedure, rotations among all orbitals are

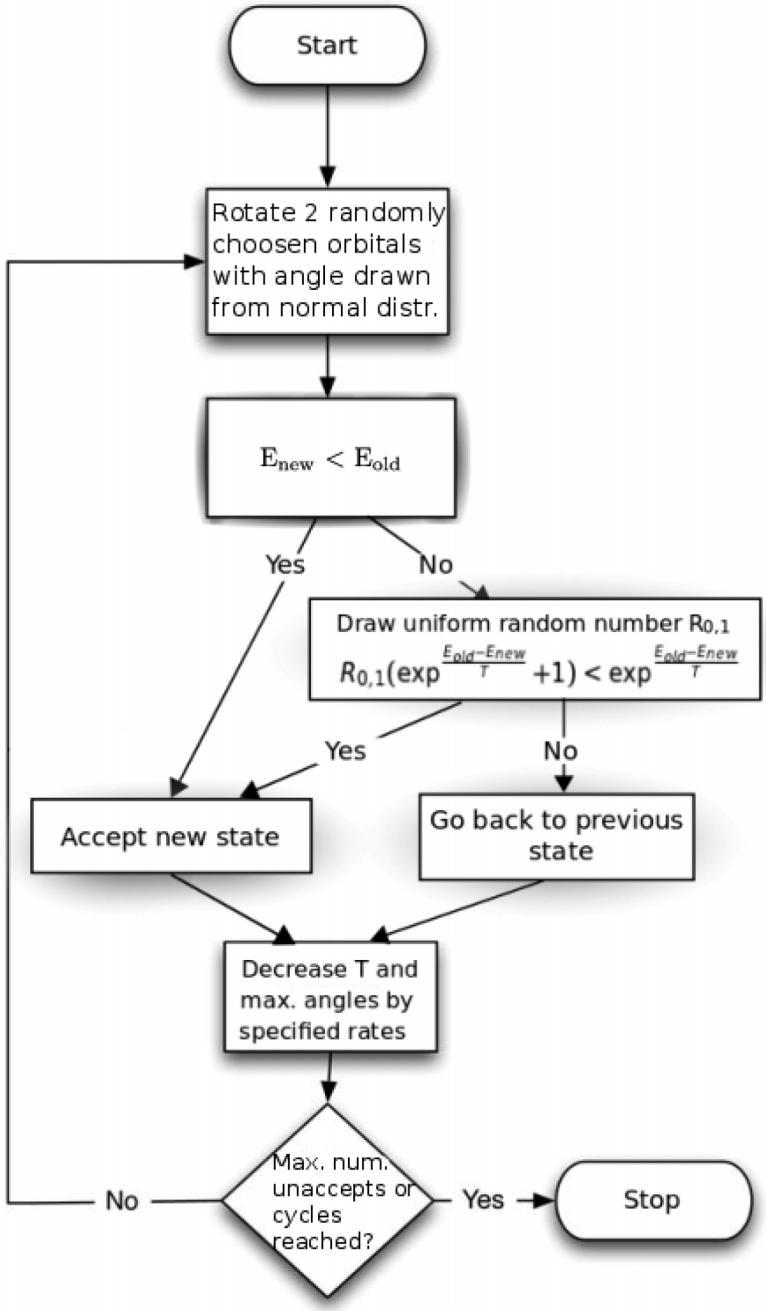

FIG. 2. The work flow of the simulated annealing (SA) orbital optimisation procedure for CI methods as implemented for this paper.

allowed thereby permitting symmetry breaking. Results with this basis are denoted as OO-c1.

2. Seniority based orbital optimisation

For large systems, SA is no longer viable. Some of us have previously shown[12] that a promising basis is the one that minimises the seniority number (Eq. (2)) of a FCI wave function. Unfortunately, the computational cost of a FCI calculation severely limits the applicability of this method. Here, we propose to use an orbital basis that minimises the seniority number of a wave function that scales more favorably, e.g., CISD.

Our procedure to minimise the seniority number of a wave function is a very fast converging iterative process based on the algorithm of Subotnik *et al.*,[23] originally introduced for the determination of localised molecular orbitals such as Edmiston-Ruedenberg orbitals.[24] It follows from Eq. (2) that if the partial trace of the spin summed second order reduced density matrix is maximised, the seniority number of the total wave function is minimised. Our adaptation of the procedure of Subotnik *et al.*[23] to minimise the seniority number proceeds as follows.[12]

1. Start with a set of orthonormal orbitals, e.g., the RHF molecular orbitals.
2. For $k \geq 0$ (k indicates the number of cycles), determine the 2-RDM for which we want to minimise the seniority number.
3. Construct the matrix $R^{(k)}_{ji} = \Gamma^{(k)}_{ji,ii}$.

4. Construct the unitary transformation $U^{(k+1)} = R^{(k)}\left[\left(R^{(k)}\right)^{\dagger} R^{(k)}\right]^{-\frac{1}{2}}$.
5. Transform the current orbitals to the new basis with the unitary matrix $U^{(k+1)}$.
6. Set $k = k + 1$, repeat steps 2-6 until $R^{(k)}$ is sufficiently close to a symmetric matrix and the process has converged.

The matrix U in step 4 is guaranteed to be unitary through the polar decomposition of a square complex matrix.[25] The orbitals produced by minimising the seniority number of a FCI wave function are denoted by the labels Mmin and Mmin-c1, depending, respectively, on whether only rotations between orbitals of the same irreducible representation are considered or symmetry breaking is allowed. If the seniority number is minimised using a wave function other than FCI, a subscript is added to denote the wave function used (e.g., $\text{Mmin}_{\text{CISD}}$ when the seniority of a CISD wave function is minimised without symmetry breaking).

III. RESULTS AND DISCUSSION

In the following, both the orbital optimisation algorithms and newly described DOCI methods are tested for a set of small molecules with emphasis on their dissociation curves for the ground state. In Section III A, the bond breaking curve of BeH_2 through linear symmetric stretching is examined with focus on the effect of different bases on the one hand (Subsection III A 1) and the effect of extending DOCI with non-seniority conserving excitations on the other hand (Subsection III A 2). As in both cases, the OO basis is used, only a minimal basis set is considered. In Section III B, we report on the performance of truncated DOCI methods (Subsection III B 1) and truncated DOCI supplemented with non-seniority conserving excitations (Subsection III B 2). Due to the fact that the truncation reduces the computational cost significantly while adding only limited non-seniority conserving excitations, we report results obtained using larger basis sets thereby allowing more insight into dynamic electron correlation effects.

A. Orbital optimisation and dynamic correlation in BeH_2

1. Basis dependence of DOCI wave functions and energies

We first describe the impact of the chosen orthonormal orbital basis on the DOCI energy in case of bond breaking in BeH_2 through linear symmetric stretching. This small molecule is computationally tractable for FCI methods and has significant multireference character at bond breaking, making it an ideal test for proof of principle calculations. Table I reports DOCI energies using the STO-3G atomic basis set for orbitals optimised with the SA approach (OO and OO-c1) and for the seniority number minimising ones (Mmin and Mmin-c1 derived from both FCI and CISD), along with the DOCI energy obtained using RHF based MOs. Although the STO-3G basis set has its shortcomings due to its size, it still captures the essence of the physics as the shape of the potential energy curve for BeH_2 remains similar for larger basis sets (see Figs. 7(a) and 10). The lowest energies, obtained using the OO-c1 basis arising from the energy driven global optimisation, can be considered as reference values.

Figs. 3(a) and 3(b) show the DOCI potential energy curves in the selected bases with the RHF and FCI curves as references. Fig. 4 depicts DOCI energy differences for the different bases considered.

Table I and Figs. 3 and 4 illustrate several important points. First, the MO basis is found to perform quite well for small interatomic distances compared to the computationally much more expensive OO basis. Beyond an internuclear distance of 1.66 Å, the energies start to differ dramatically with differences going up to 120 mE_h at 2.77 Å (see Fig. 4(a)). Optimising the orbitals is therefore of utmost importance at longer bond distances although the differences decrease again at still longer distances (see Fig. 4(a)). Fig. 4(b) shows that the energy obtained from the Mmin basis lies much closer to the OO energy over a larger range of interatomic distances, with differences up to only 38 mE_h near 2.45 Å. Moreover, the difference between energies obtained with the $\text{Mmin}_{\text{CISD}}$ and the Mmin bases is rather small as can be seen from Table I. Fig. 3(c), which depicts the overlap of the DOCI wave function

TABLE I. STO-3G DOCI energy values and differences for the symmetric stretch of BeH_2 using different orthonormal bases. R is the length of the Be–H bonds.

	DOCI energy/E_h								
R (Å)	MO	OO	Mmin	$\text{Mmin}_{\text{CISD}}$	$\text{Mmin}_{\text{CISD}}$–OO	OO-c1	Mmin-c1	$\text{Mmin}_{\text{CISD}}$-c1	$\text{Mmin}_{\text{CISD}}$-c1–OO-c1
0.86	−15.295 973	−15.296 475	−15.296 470	−15.296 465	0.000 010	−15.299 640	−15.294 537	−15.294 546	0.005 094
1.02	−15.490 483	−15.490 920	−15.490 914	−15.490 907	0.000 013	−15.496 264	−15.489 413	−15.489 420	0.006 844
1.34	−15.578 003	−15.578 459	−15.578 436	−15.578 419	0.000 039	−15.590 358	−15.590 139	−15.590 199	0.000 159
1.66	−15.510 719	−15.511 515	−15.511 405	−15.511 344	0.000 170	−15.533 722	−15.533 153	−15.533 328	0.000 393
1.98	−15.402 028	−15.404 541	−15.403 776	−15.403 513	0.001 028	−15.440 935	−15.439 646	−15.439 380	0.001 555
2.13	−15.347 166	−15.353 874	−15.350 794	−15.350 214	0.003 660	−15.395 504	−15.391 057	−15.391 663	0.003 841
2.29	−15.297 031	−15.328 067	−15.306 903	−15.305 553	0.022 514	−15.354 530	−15.342 597	−15.342 969	0.011 561
2.45	−15.255 160	−15.325 976	−15.288 084	−15.282 966	0.043 011	−15.325 976	−15.288 084	−15.282 966	0.043 011
2.61	−15.225 362	−15.328 124	−15.307 317	−15.288 895	0.039 229	−15.328 124	−15.307 317	−15.288 895	0.039 229
2.77	−15.210 719	−15.330 642	−15.325 165	−15.307 031	0.023 611	−15.330 642	−15.325 165	−15.307 031	0.023 611
3.09	−15.226 272	−15.334 189	−15.333 775	−15.330 958	0.003 231	−15.334 189	−15.333 775	−15.330 958	0.003 231

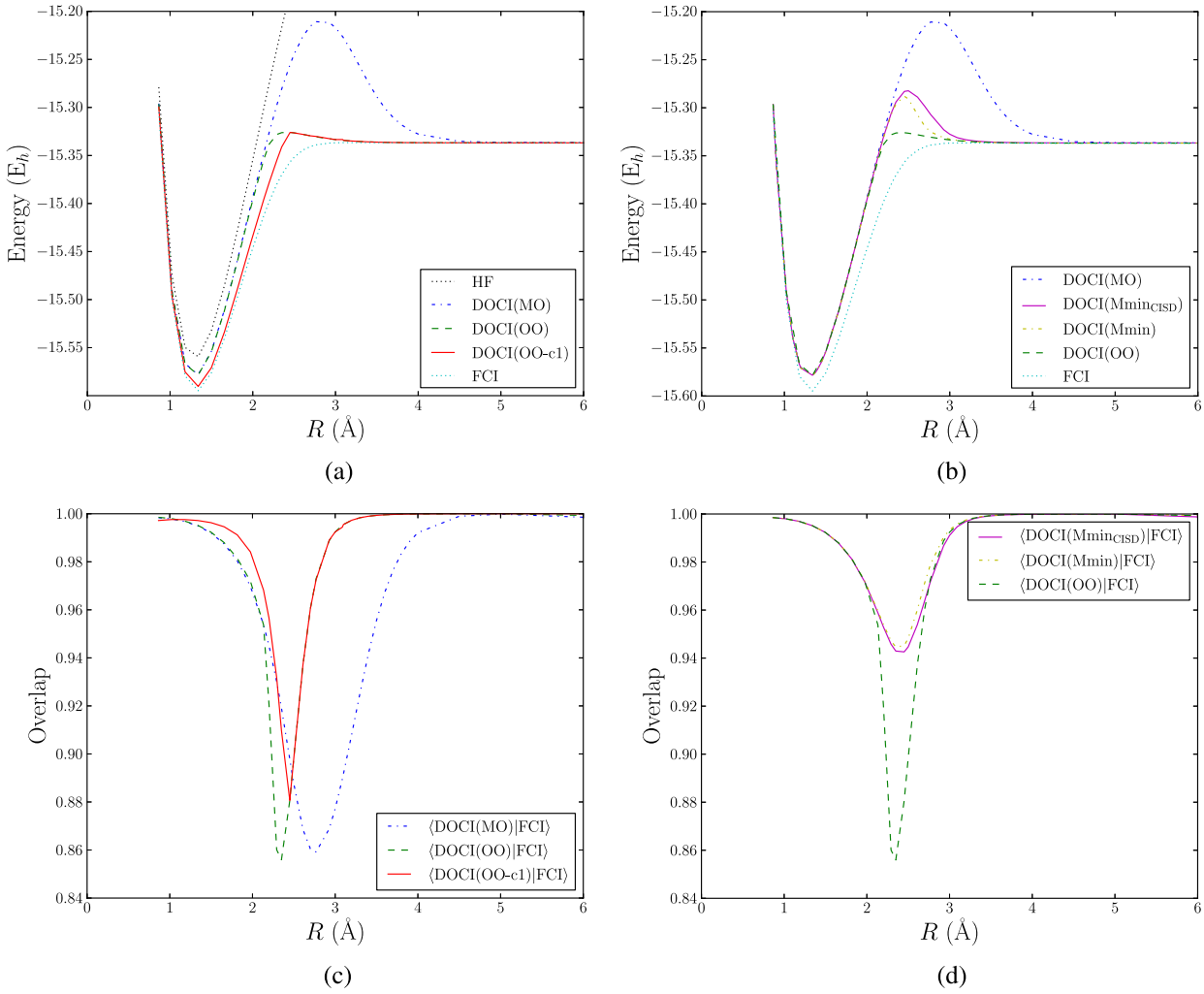

FIG. 3. Symmetric stretch potential energy curves as a function of the Be–H distance (R) in BeH_2 for the (a) RHF, DOCI(MO), DOCI(OO), DOCI(OO-c1), and FCI wave functions, and (b) DOCI(MO), DOCI(Mmin$_{CISD}$), DOCI(Mmin), DOCI(OO), and FCI wave functions in the STO-3G atomic basis set. (c) Overlap between the STO-3G DOCI and FCI wave functions in the MO, OO, and OO-c1 bases. (d) Overlap of the STO-3G DOCI and FCI wave functions in the OO, Mmin, and Mmin$_{CISD}$ bases.

with the FCI wave function, illustrates the deficiencies of the DOCI wave function in the MO, OO, and OO-c1 basis to approximate the FCI wave function around a bond distance of 2.45 Å.

Symmetry breaking has an effect at slightly shorter bond lengths than those where the highest deviations between the Mmin and OO based energies occur (see Fig. 4(c)). As expected for a variational method, symmetry-breaking may lower the energy. Note that the sharp angle in the DOCI(OO-c1) energy curve is not due to states crossing but due to a sudden change in the basis. A similar finding was reported previously by Bytautas *et al.*[4] for H_8. In the case of the OO-c1 versus OO basis, symmetry breaking leads to a maximum energy lowering of 42 mE$_h$ at an internuclear distance of 2.13 Å. Such an effect does not necessarily occur for the Mmin and Mmin-c1 bases. Here, symmetry breaking may result in higher energies especially at short bond lengths. Although counterintuitive, this is not in stride with the minimisation condition behind the Mmin procedure, as this procedure searches for a minimum in *seniority number*, rather than in *energy*. By breaking the symmetry, the method can better pair the electrons, irrespective of the energy. Still, the energy increase is marginal with a maximum of 2 mE$_h$ while for the vast majority of the energy curve, symmetry breaking still lowers the energy.

As a whole, for most of the interatomic distances, the seniority-number minimising basis is a good alternative to the energy based optimised orbitals with the computationally cheap Mmin$_{CISD}$ basis also performing rather well.

2. Dynamic correlation and hybrid DOCI wave functions

It is clear from Table I and Figs. 3(a) and 3(b) that one can distinguish between three different regimes during bond breaking. At small bond distances, Hartree-Fock theory yields a fairly good wave function. Indeed, near the equilibrium bond length, the RHF determinant is the most important determinant in the FCI expansion. This regime extends well across the valley of the FCI potential minimum. This is consistent with the observation that, in this regime, the FCI natural orbitals have occupations roughly zero or two (see Fig. 5).

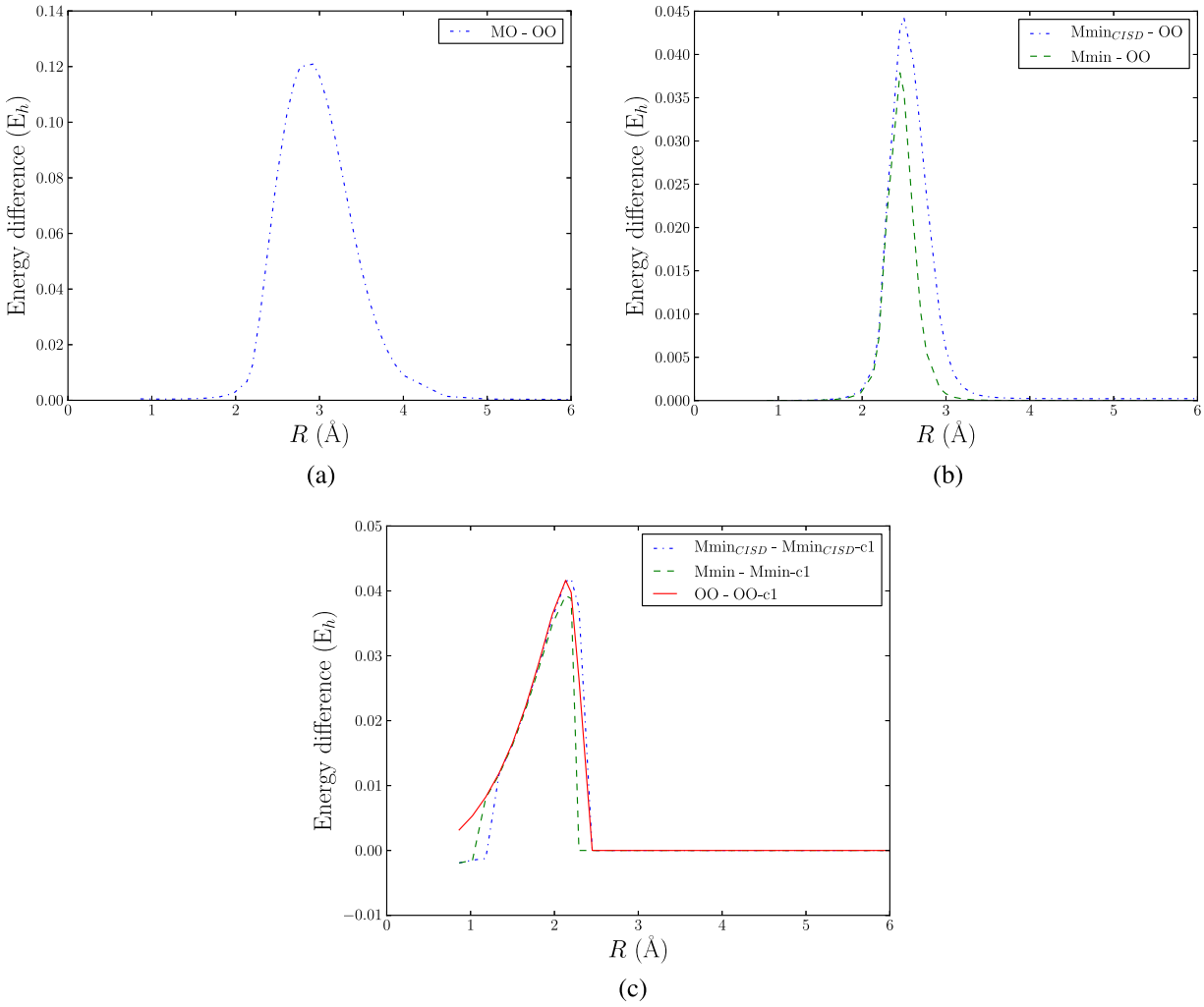

FIG. 4. STO-3G DOCI energy differences between different bases as a function of the Be–H distance (R) in BeH_2. (a) Effect of energy based orbital optimisation, (b) comparison between energies obtained with the energy optimised (OO) and Mmin and $Mmin_{CISD}$ seniority optimised orbitals, and (c) effect of symmetry breaking.

As soon as bond breaking starts, dynamic correlation becomes increasingly important, while farther towards dissociation, static correlation gains importance. The interval where in BeH_2 dynamic correlation dominates corresponds approximately to [1.8 Å, 2.5 Å]. In this interval, the occupation number of the natural orbitals closest to the Fermi level (between the highest occupied molecular orbital (HOMO) and lowest unoccupied molecular orbital (LUMO) levels from Hartree-Fock) starts to differ from zero or two, although the complete smearing out of occupation numbers as in the strong correlation limit does not occur.

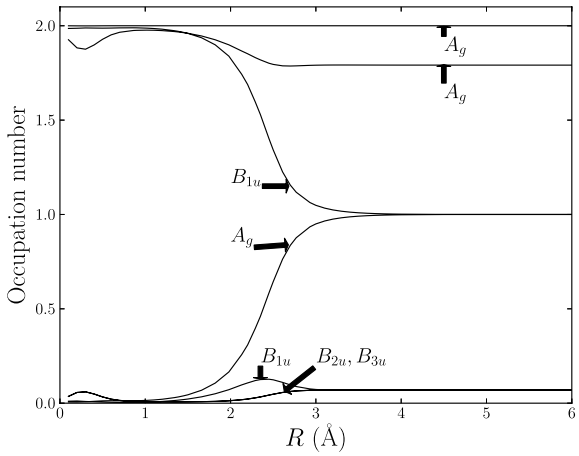

FIG. 5. Occupation numbers of the STO-3G FCI natural orbitals as a function of the Be–H bond length (R) for the symmetric bond stretching of BeH_2. The symmetry labels used are based on the D_{2h} Abelian point group used in the calculations.

In the so-called static correlation regime, it is no longer possible to find a good single reference approximation to the general wave function, e.g., the RHF energy deviates strongly from the FCI energy (see Fig. 3(a)). This is well reflected in the fact that many more natural orbitals have significant occupation numbers, and hence, the distinction between occupied and virtual orbitals vanishes. The strong static correlation regime is characterised by degenerate strongly occupied molecular orbitals. The particular structure of the DOCI wave function turns out to be very suitable to describe this, since the DOCI wave function is a complete CI expansion in terms of electron pairs.[4]

As can be observed from Fig. 3(a), the peculiar hump in the DOCI(MO) potential energy curve within the dynamic

correlation regime reflects the difficulties of the DOCI wave function to describe dynamic correlation properly in the MO basis. The hump itself is not an artefact of the minimal basis set as DOCI(MO) calculations using the 6-31G and cc-pVDZ basis set also show a similar feature (see Figs. 7(a) and 10). Using the OO and OO-c1 bases reduces the extent of the problem but does not completely alleviate it. As the importance of dynamic correlation increases, the FCI and DOCI energies differ more. Once static correlation becomes more important than dynamic correlation, the particular structure of the DOCI wave functions causes this difference to decrease. The problems of the DOCI wave function in the dynamic correlation regime can be solved by applying multi-reference perturbation theory[26,27] or by adding extra determinants in its expansion.[28]

To better understand the correspondence between the DOCI wave function in different bases and the FCI wave function, Fig. 3(c) shows the overlap between both wave functions in the MO, OO, and OO-c1 bases in the STO-3G basis set. This figure illustrates the failure of DOCI in the dynamic correlation regime. At shorter bond distances and near equilibrium, DOCI performs well as it basically acts as a correction scheme for the dominant RHF ground-state. At large internuclear separation, in the strong correlation limit, we again find high overlap between DOCI and FCI wave functions. In the dynamic correlation regime, the overlap is much lower with a minimum of about $|\langle \text{DOCI(OO)}|\text{FCI}\rangle|^2 = (0.86)^2 = 0.74$ around 1.7 Å, pointing out that the FCI wave function carries important contributions from configurations outside the DOCI space. Note that orbital optimisation from the MO to the OO basis does reduce the range of bond distances where these problems occur but does not eliminate the effects of dynamic correlations completely. Also note that the poor overlap persists, however shifted towards shorter R. Remarkably, the overlap between the Mmin or $\text{Mmin}_{\text{CISD}}$ based DOCI wave function and the FCI wave function is significantly better than the OO based one (see Fig. 3(d)) although the Mmin and $\text{Mmin}_{\text{CISD}}$ based DOCI wave functions do not yield the lowest energies (see Fig. 3(b)). This is consistent with the previous reports[29,30] that energy minimisation alone does not guarantee finding the wave function most similar to the FCI one. The OO basis is designed to lower the energy and will do so by focussing on those determinants that assist it maximally whereas the treatment of (incipient) static correlation is less important. The Mmin basis, on the other hand, capitalises maximally on zero seniority determinants typically important to properly treat static correlation. Breaking the symmetry as in the OO-c1 basis does improve the quality of the wave function in the dynamic correlation regime. Note that Fig. 3(c) shows that even the DOCI(MO) wave function has significantly higher overlap with the FCI wave function than the DOCI(OO) one for 2.1 Å $\leq R \leq$ 2.5 Å. To conclude, one should be cautious when performing energy optimisation, as this process may reduce the overlap with the exact wave function, even if a variational method is used (see Fig. 3(c)).

Although the Mmin and $\text{Mmin}_{\text{CISD}}$ bases significantly improve the overlap of the DOCI wave function with the FCI wave function in the dynamic correlation regime compared with the OO, and even OO-c1 orbitals, there still remains a small discrepancy at intermediate bond distances (with a minimum of $|\langle \text{DOCI(Mmin)}|\text{FCI}\rangle|^2 = (0.94)^2 = 0.88$). In an attempt to improve the DOCI wave function, extra determinants from the CIS and CISD spaces are now added to the Slater determinant expansion. This leads to the hybrid (CIS ∪ DOCI) and (CISD ∪ DOCI) wave functions, respectively. Fig. 6 shows the overlap between the DOCI, (CIS ∪ DOCI), and (CISD ∪ DOCI) wave functions and the FCI one, for the MO (Fig. 6(a)) and OO bases (Fig. 6(b)). These figures show that the overlap improves dramatically upon inclusion of broken pair excitations, again consistent with the described importance of dynamic correlation. This agrees with the fact that second order perturbation theory (MP2) improves on the description of dynamic correlation by including doubly excited determinants both inside and outside DOCI space. The advantage of methods that unite DOCI and truncated CI spaces is that, compared to FCI, the number of determinants remains smaller. For instance, in the case of BeH_2, the number of determinants required in the STO-3G (CISD ∪ DOCI) and FCI methods is 227 and 1225, respectively, while the overlap between the (CISD ∪ DOCI)

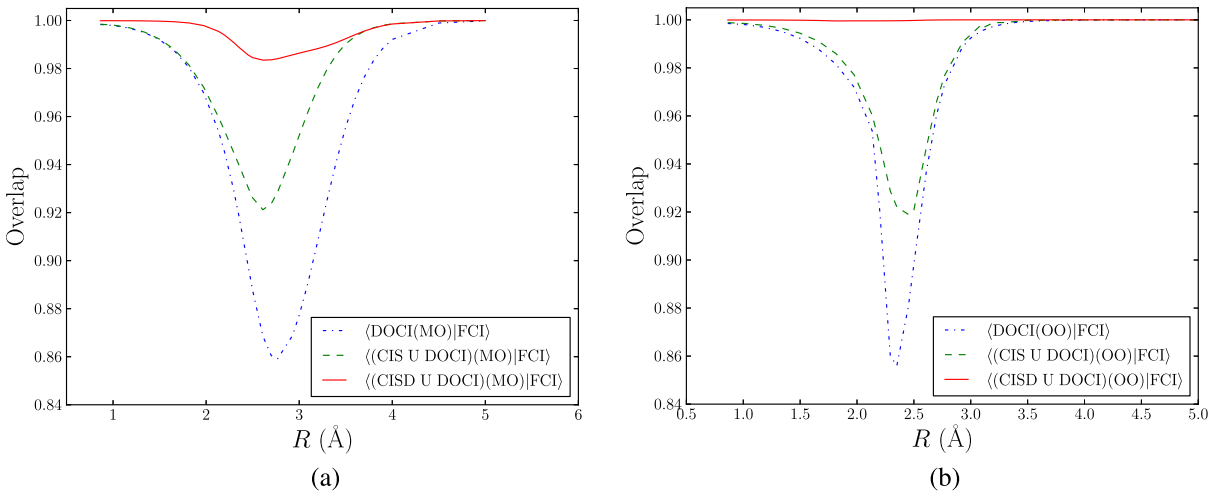

FIG. 6. Overlap of the DOCI, (CIS∪DOCI), and (CISD∪DOCI) wave functions with the FCI wave function in the (a) MO and (b) OO bases for the BeH_2 molecule in the STO-3G atomic basis set. R is the distance of the stretched Be–H bonds.

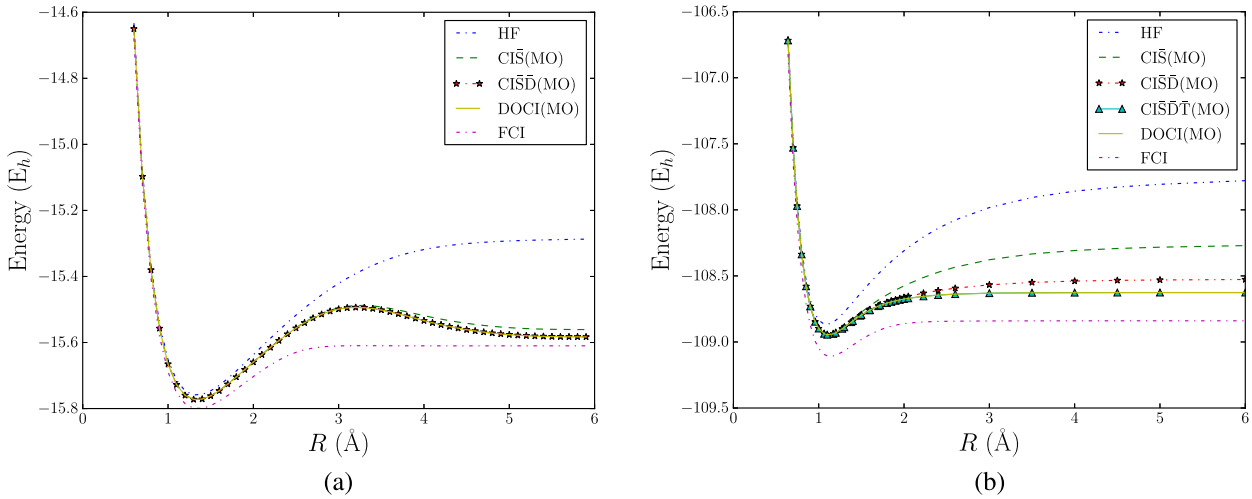

FIG. 7. Potential energy curves for the symmetric stretch of (a) linear BeH_2 and (b) the N_2 molecule, at the RHF, CIS̄, CIS̄D̄, DOCI, and FCI levels of theory with 6-31G based MO orbitals. For N_2, the CIS̄D̄T̄ method is also included. R is the length of the stretched bond.

and FCI wave functions remains consistently large over the entire bond-breaking curve (see Fig. 6(b)).

B. New approximate DOCI methods

1. Truncated DOCI

DOCI is a powerful method for the description of static correlation, but unfortunately still scales exponentially as it is a complete CI method albeit in electron-pair space. As in standard one-electron excitation based CI, it is therefore of interest to examine whether a truncated DOCI approach is viable. Henceforth, truncated DOCI wave functions will be denoted by CIS̄, CIS̄D̄, etc., for a single reference closed-shell determinant supplemented with either all single electron-*pair* excitations or all single and double electron-*pair* excitations, respectively. DOCI then corresponds to CIS̄D̄T̄Q̄ . . . $\bar{K}$. To analyse how much information of the DOCI wave function remains in the truncated DOCI wave functions, the overlap between both is computed as well as the corresponding energies during the bond breaking of the N_2 molecule and the symmetric stretch of the BeH_2 molecule (see Figs. 7–9). The MO basis obtained from a Hartree-Fock calculation with the 6-31G atomic basis set is used for all analyses in this subsection as the MO basis is the commonly used reference for one-electron excitation based CI.

Fig. 7 shows that the truncated DOCI methods yield energies fairly close to the DOCI result although the required level of truncation varies (N_2 requiring up to three electron-pair excitations whereas for the other molecule, CIS̄D̄ largely suffices). Note that Fig. 7(a) shows a clear hump in the DOCI(MO) energy, reminiscent of what was found in Fig. 3(a) where a minimal basis set was used. The overlap of the truncated DOCI and DOCI wave functions is depicted in Fig. 8. It is clear that at small and intermediate bond distances, single electron-pair excitations alone are able to describe the DOCI wave function with high accuracy. However, at larger bond distances, single and double electron-pair excitations are needed for BeH_2, and even single, double, and triple electron-pair excitations must be considered for N_2. There the overlap with DOCI is almost perfect over the entire range of distances. Finally, Fig. 9 shows the sum of the squares of the coefficients

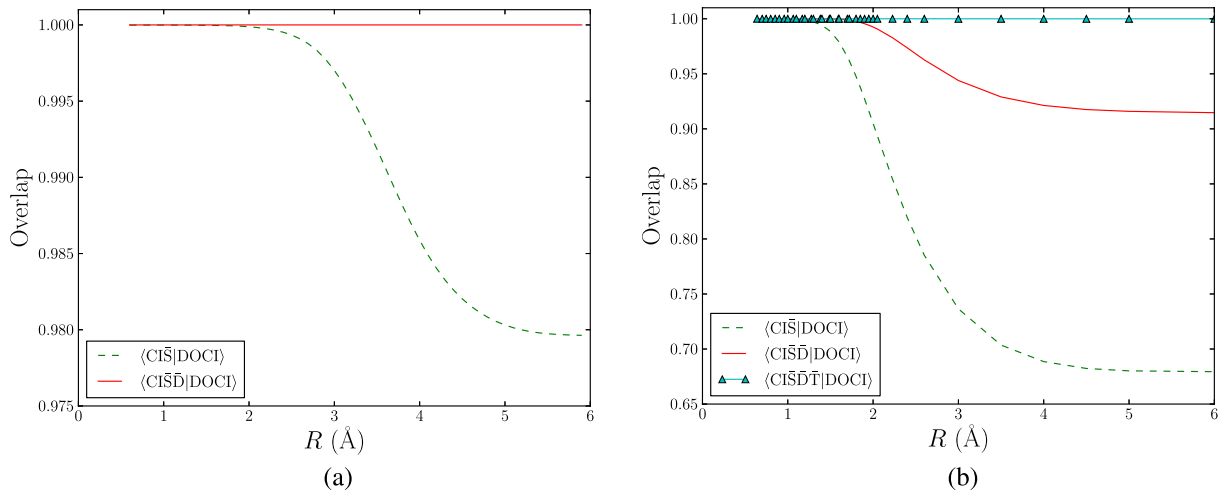

FIG. 8. Overlap of the CIS̄ and CIS̄D̄ wave functions with the DOCI one using 6-31G based MO orbitals for the symmetric stretch of (a) linear BeH_2 and (b) the N_2 molecule. For N_2, the overlap with the CIS̄D̄T̄ wave function is also included. R is the length of the stretched bond.

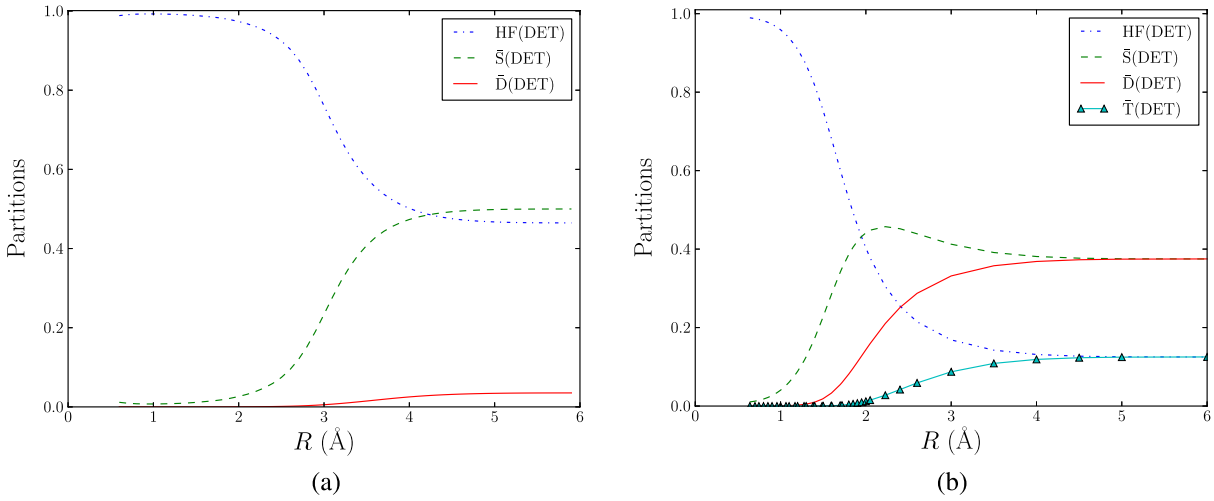

FIG. 9. Sums of squared Slater determinant coefficients of different excitation levels in the DOCI wave function using 6-31G based MO orbitals for the symmetric stretch of (a) linear BeH_2 and (b) the N_2 molecule. R is the length of the stretched bond.

of the RHF determinant (RHF(DET)) and all single ($\bar{S}$(DET)) and double ($\bar{D}$(DET)) electron-pair excited determinants of the DOCI wave function for the BeH_2 and N_2 molecules. For N_2, also the sum of the squares of the coefficients of triple electron-pair excited determinants ($\bar{T}$(DET)) is included. This reflects the amount of information of the DOCI wave function that is contained in its parts. The figure confirms the trends expected from the earlier findings: RHF performs well at short bond distances and the contributions of higher excited determinants to the DOCI wave function become larger as the bond distance increases.

2. Approximate hybrid DOCI

On the one hand, hybrid methods based on the addition of disjoint determinant spaces to supplement the DOCI wave function, as described above in Section III A 2 and previously by some of us,[28] still scale less than desirable with system size. On the other hand, fairly good approximations to DOCI are possible by truncating DOCI to lower excitation levels only, as put forward in Section III B 1. Combining truncation of DOCI and extending it with electron-pair breaking determinants from standard one-electron excitation based CI, we come naturally to approximate methods that incorporate some lower *one-electron* excitations of a reference along with electron-*pair excited* determinants from DOCI. Examples of such combinations are the CISD$\bar{D}$ and CISD$\bar{D}\bar{T}$ levels of theory, where CISD is augmented with two electron-*pair* excited determinants or two and three electron-*pair* excited determinants, respectively. CISD$\bar{D}$ is therefore a subset of CISDQ where, among the quadruple excitations, only those determinants are withheld that correspond to excitations of two electron-*pairs*. In this way, it is possible to add many relevant higher excitations in a computationally feasible way. This can be combined with the seniority number minimising basis which is obtained through a fast iterative process and yet improves the description of the electronic structure in the static correlation regime (see Fig. 10). Seniority minimisation using a CISD wave function allows a further gain in speed compared to seniority number minimising directly in the approximate hybrid space as the CISD wave function contains fewer determinants compared to most approximate hybrid methods. The advantage of the present type of approximate hybrid methods is thus that the computational cost scales much more favourably with system size (in this case polynomial scaling, see Table II) providing accurate energies at much smaller cost (e.g., CISD$\bar{D}$ for BeH_2 in the cc-pVDZ basis set contains 5986 Slater determinants compared to the 4 096 576 Slater determinants included in the FCI wave function).

Fig. 10 shows the symmetric stretching potential energy curve for BeH_2 obtained using the CI$\bar{S}\bar{D}$(Mmin$_{CISD}$), DOCI (Mmin$_{CISD}$), CISD(MO), CISD$\bar{D}$(MO), and CISD$\bar{D}$ (Mmin$_{CISD}$) methods for the cc-pVDZ atomic basis set, and the FCI and coupled cluster CCSD(T) methods as references. It shows the improved description of the dissociation limit by adding extra pair excitations to the CISD wave function and the enhancing effect of the Mmin$_{CISD}$ basis on those pair

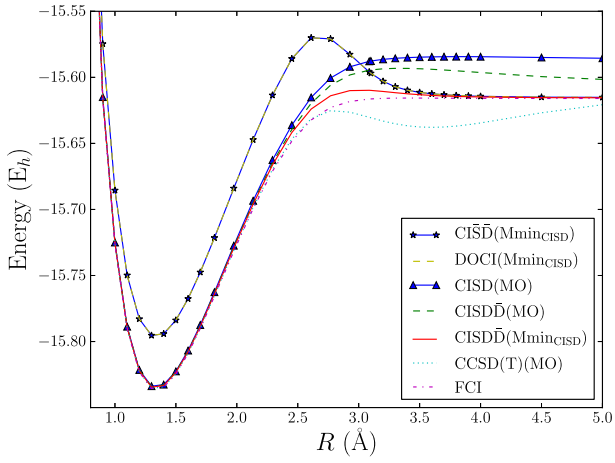

FIG. 10. Potential energy curve for symmetric stretching of BeH_2 using the CI$\bar{S}\bar{D}$, DOCI, and CISD$\bar{D}$ methods in the seniority number minimising basis (Mmin$_{CISD}$) and CISD, CISD$\bar{D}$, and CCSD(T) methods in the MO basis with FCI as reference. All calculations were performed with the cc-pVDZ atomic basis set. R denotes the Be–H bond length.

TABLE II. Number of determinants, N_{det}, for a selection of discussed methods for BeH_2 and N_2 in cc-pVDZ, together with the percentage of the FCI determinants contained.

	BeH_2		N_2	
Methods	N_{det}	$\frac{N_{det}}{N_{det}(FCI)}100$	N_{det}	$\frac{N_{det}}{N_{det}(FCI)}100$
CIS̄	64	0.002	148	1.100×10^{-8}
CIS̄D̄	694	0.017	4 558	3.250×10^{-7}
CIS̄D̄T̄	2 024	0.049	51 108	3.645×10^{-6}
DOCI	2 024	0.049	1 184 040	8.446×10^{-5}
CISD	5 356	0.131	30 724	2.192×10^{-6}
CISDD̄	5 986	0.146	35 134	2.506×10^{-6}
CISDD̄T̄	7 316	0.179	81 684	5.826×10^{-6}
(CISD∪DOCI)	7 316	0.179	1 214 616	8.664×10^{-5}
FCI	4 096 576	100	1 401 950 721 600	100

excitations. Both CISDD̄ curves lie fairly close to the FCI one but with still a relevant improvement from using the seniority number minimising basis ($Mmin_{CISD}$). The remaining errors lie in the mE_h scale. Note that CCSD(T)[31,32] (in the MO basis) does not perform well when static correlation is important. The most significant deviation of the CISDD̄($Mmin_{CISD}$) energy from the FCI one is in the regime where dynamic correlation is dominant. This is most likely a remnant of the fact that the $Mmin_{CISD}$ basis does not yield very good energies in this regime. Note also that CISDD̄(MO) still results in a hump somewhat reminiscent of that observed earlier albeit now at larger distances and that it is much smaller. This is thanks to the inclusion of the one electron and unpaired two electron excitations that assist in properly accounting for dynamic correlation. The most important observation in Fig. 10 is that the CISDD̄($Mmin_{CISD}$) energies follow closely the CISD(MO) energy curve wherever the latter method lies close to FCI and that it lies very close to the DOCI($Mmin_{CISD}$) results towards dissociation. In the area between both regimes, the energy error with respect to FCI is the smallest among all methods tested.

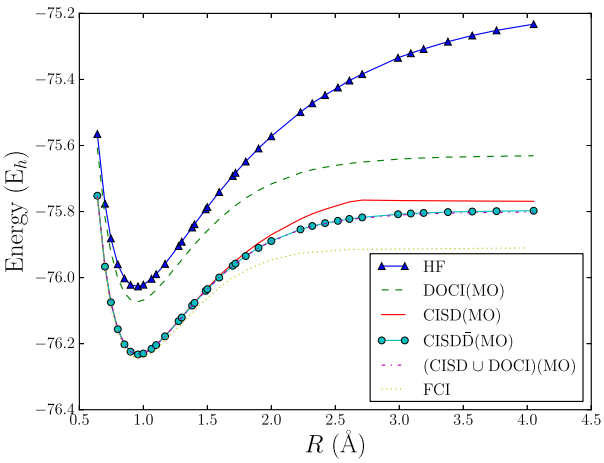

FIG. 11. Potential energy curve for symmetric stretching of the H–O bonds in H_2O using the RHF, DOCI, CISD, (CISD∪DOCI), CISDD̄, and FCI methods using MO obtained from the cc-pVDZ atomic basis set. R denotes the H–O bond length.

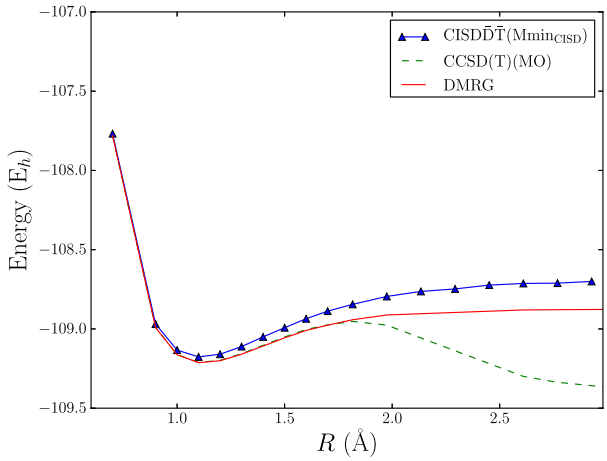

FIG. 12. Potential energy curve for the N_2 dimer for CCSD(T) in the MO basis, CISDD̄T̄ ($Mmin_{CISD}$, CAS(10,18)), and DMRG[14,15] using the cc-pVDZ atomic basis set. R is the interatomic distance.

Fig. 11 shows the potential energy curve of the symmetric stretching of the H_2O molecule at several levels of theory for the cc-pVDZ atomic basis set. It shows that the (CISD ∪ DOCI) and CISDD̄ potential energy curves are indistinguishable over the entire bond length range, and that both methods improve significantly on CISD in the static correlation regime. In general, for systems with not too many electrons, such as H_2O, the difference in energy between this approximate hybrid (CISDD̄) method and the hybrid method (CISD ∪ DOCI) is negligible.

Finally, Fig. 12 shows the potential energy surface for N_2 in the cc-pVDZ basis. The methods compared are CCSD(T) in the MO basis and the CISDD̄T̄ ($Mmin_{CISD}$, CAS(10,18)). Density matrix renormalisation group (DMRG)[14,15] energies with FCI accuracy are added as a reference. CCSD(T) performs better at equilibrium and intermediate bond distances, but the approximate hybrid method outperforms CCSD(T) in the dissociation limit. The basic implementation of our routines made us resort to an active space of 10 electrons in 18 orbitals for N_2 in cc-pVDZ. This was probably the reason why CISDD̄T̄ ($Mmin_{CISD}$) is less accurate at equilibrium (see Fig. 12).

IV. CONCLUSIONS

The orbital dependence of DOCI wave functions and energies has been scrutinised. This is done first by comparing the DOCI energies, obtained using different bases, among each other and with reference FCI energies, and second by studying wave function overlaps. The straightforward use of molecular orbitals often results in rather poor DOCI energies and wave functions. To ameliorate this, a technique based on SA is described to search for the optimal single-particle basis that globally minimises the energy. This approach is found to significantly reduce the energy difference between DOCI and the FCI wave function, especially in the dynamic correlation regime. The SA approach is computationally, however, too costly and it is shown that an orbital optimisation algorithm minimising the seniority of the CISD wave function is an

efficient alternative yielding nearly as good results, especially in the static correlation regime. Moreover, this basis often results in better overlap with the reference wave functions despite a slightly higher energy than that obtained with the SA optimised basis. This shows that better agreement in wave function and energy does not always coincide.

Next, a set of new methods related to DOCI has been introduced. The first type of methods is truncated DOCI methods where the level of pair excitations considered is reduced to, e.g., only one pair and two pairs, much like in one electron excitation based CIS, CISD, etc. The results obtained using this method show that static correlation, as present near bond dissociation, is already captured with a limited level of excitations. Dynamic correlation is not properly accounted for at this level. In order to properly describe dynamic correlation, in the second set of methods, these truncated DOCI methods are supplemented with determinants obtained from unpaired electron excitations resulting in methods that combine, e.g., one and two pair excitations from the determinants contained in DOCI with all unpaired one and two electron excitations. The resulting methods scale polynomially with system size, making them computationally attractive and affordable for larger systems.

ACKNOWLEDGMENTS

M.V.R., W.P., S.D.B., P.B., and D.V.N. are members of the QCMM alliance Ghent-Brussels. M.V.R., W.P., S.D.B., and P.B. acknowledge the support from the Research Foundation Flanders (FWO Vlaanderen). P.B. and D.R.A. acknowledge the FWO Vlaanderen and the Ministerio de Ciencia, Tecnología e Innovación Productiva (Argentina) for collaborative research grant VS.0001.14N. D.R.A. acknowledges the Universidad de Buenos Aires (Argentina) and the Consejo Nacional de Investigaciones Científicas y Técnicas (Argentina) for research Grant Nos. UBACYT 20020100100197, PIP 11220090100061, and PIP 11220130100377CO. A.T. and L.L. acknowledge the Universidad del Pais Vasco (Spain) for research Grant Nos. GIU12/09 and UFI11/07. The computational resources (Stevin Supercomputer Infrastructure) and services used in this work were provided by the VSC (Flemish Supercomputer Center), funded by Ghent University, the Hercules Foundation and the Flemish Government—department EWI.

[1]A. Szabo and N. S. Ostlund, *Modern Quantum Chemistry: Introduction to Advanced Electronic Structure Theory* (Macmillan, New York, 1982).
[2]T. Helgaker, P. Jørgensen, and J. Olsen, *Molecular Electronic-Structure Theory* (Wiley, Chichester, 2000).
[3]P. Ring and P. Schuck, *The Nuclear Many-Body Problem* (Springer-Verlag, 1980).
[4]L. Bytautas, T. M. Henderson, C. A. Jiménez-Hoyos, J. K. Ellis, and G. E. Scuseria, J. Chem. Phys. **135**, 044119 (2011).
[5]D. R. Alcoba, A. Torre, L. Lain, G. E. Massaccesi, and O. B. Oña, J. Chem. Phys. **140**, 234103 (2014).
[6]P. R. Surjan, "Correlation and localization," Top. Curr. Chem. **203**, 63 (1999).
[7]P. A. Limacher, P. W. Ayers, P. A. Johnson, S. De Baerdemacker, D. Van Neck, and P. Bultinck, J. Chem. Theory Comput. **9**, 1394 (2013).
[8]T. Stein, T. M. Henderson, and G. E. Scuseria, J. Chem. Phys. **140**, 214113 (2014).
[9]P. A. Johnson, P. W. Ayers, P. A. Limacher, S. De Baerdemacker, D. Van Neck, and P. Bultinck, Comput. Theor. Chem. **1003**, 101 (2013).
[10]W. Poelmans, M. Van Raemdonck, B. Verstichel, S. De Baerdemacker, A. Torre, L. Lain, G. E. Massaccesi, D. R. Alcoba, P. Bultinck, and D. Van Neck, "Variational optimization of the second-order density matrix corresponding to a seniority-zero configuration interaction wave function," J. Chem. Theory Comput. (to be published).
[11]S. Kirkpatrick, C. D. Gelatt, and M. P. Vecchi, Science **220**, 671 (1983).
[12]D. R. Alcoba, A. Torre, L. Lain, G. E. Massaccesi, and O. B. Oña, J. Chem. Phys. **139**, 084103 (2013).
[13]J. M. Turney, A. C. Simmonett, R. M. Parrish, E. G. Hohenstein, F. Evangelista, J. T. Fermann, B. J. Mintz, L. A. Burns, J. J. Wilke, M. L. Abrams, N. J. Russ, M. L. Leininger, C. L. Janssen, E. T. Seidl, W. D. Allen, H. F. Schaefer, R. A. King, E. F. Valeev, S. D. Sherrill, and T. D. Crawford, WIREs: Comput. Mol. Sci. **2**, 556 (2012).
[14]S. Wouters, W. Poelmans, P. W. Ayers, and D. Van Neck, Comput. Phys. Commun. **185**, 1501 (2014).
[15]S. Wouters, W. Poelmans, S. De Baerdemacker, P. W. Ayers, and D. Van Neck, Comput. Phys. Commun. **191**, 235 (2015).
[16]R. B. Lehoucq, D. C. Sorensen, and C. Yang, "ARPACK users guide: Solution of large scale eigenvalue problems by implicitly restarted Arnoldi methods," 1997.
[17]P. A. Limacher, D. K. Taewon, P. W. Ayers, P. A. Johnson, S. De Baerdemacker, D. Van Neck, and P. Bultinck, Mol. Phys. **112**, 853 (2014).
[18]M. D. Andrade, K. C. Mundim, and A. C. Malbouisson, Int. J. Quantum Chem. **103**, 493 (2005).
[19]R. C. Raffenetti, K. Ruedenberg, C. L. Janssen, and H. F. Schaefer, Theor. Chim. Acta **86**, 149 (1993).
[20]P. E. M. Siegbahn, J. Almlöf, A. Heiberg, and B. O. Roos, J. Chem. Phys. **74**, 2384 (1981).
[21]H. J. Werner and P. J. Knowles, J. Chem. Phys. **82**, 5053 (1985).
[22]B. O. Roos, Int. J. Quantum Chem. **18**(S14), 175 (1980).
[23]J. E. Subotnik, Y. Shao, W. Z. Liang, and M. Head-Gordon, J. Chem. Phys. **121**, 9220 (2004).
[24]C. Edmiston and K. Ruedenberg, Rev. Mod. Phys. **35**, 457 (1963).
[25]G. H. Golub and C. F. Van Loan, *Matrix Computations*, 3rd ed. (The Johns Hopkins University Press, 1996).
[26]M. Kobayashi, A. Szabados, H. Nakai, and P. R. Surján, J. Chem. Theory Comput. **6**, 2024 (2010).
[27]P. A. Limacher, P. W. Ayers, P. A. Johnson, S. De Baerdemacker, D. Van Neck, and P. Bultinck, Phys. Chem. Chem. Phys. **16**, 5061 (2014).
[28]D. R. Alcoba, A. Torre, L. Lain, O. B. Oña, P. Capuzzi, M. Van Raemdonck, P. Bultinck, and D. Van Neck, J. Chem. Phys. **141**, 244118 (2014).
[29]D. H. Kobe, Phys. Rev. C **3**, 417 (1971).
[30]W. Brenig, Nucl. Phys. **13**, 363 (1957).
[31]G. D. Purvis and R. J. Bartlett, J. Chem. Phys. **76**, 1910 (1982).
[32]K. Raghavachari, G. W. Trucks, J. A. Pople, and M. Head-Gordon, Chem. Phys. Lett. **157**, 479 (1989).